Fire Safety Journal 120 (2021) 103066

Contents lists available at ScienceDirect

Fire Safety Journal

journal homepage: http://www.elsevier.com/locate/firesaf

Experimental study of fire spread through discontinuous fuels without flame contact

Leo Schneider [a], Benjamin Betting [a], Matthew Patterson [b], Nicholas Skowronski [b], Albert Simeoni [a,*]

[a] Worcester Polytechnic Institute, 100 Institute Road, Worcester, MA, USA
[b] USDA Forest Service, Northern Research Station, Morgantown, WV, USA

ARTICLE INFO

Keywords:
Forest fire
Wildland fire
Fire spread
Radiative transfer
Discontinuous fuel
Douglas fir

ABSTRACT

There is a strong need to increase the basic understanding of the propagation mechanisms in wildfires to improve the scientific tools needed for firefighting and fire prevention. This study focuses on the fire spread mechanisms by radiation. Three contiguous trees were ignited and the mechanisms leading to flame spread to a target tree were analyzed. The experiments were designed to avoid fire spread by flame contact and study how radiation heat transfer could ignite the target tree. Different measurements were performed, including heat fluxes, temperature and mass loss rate. The vegetation was characterized in details by using terrestrial laser scan reconstruction. The analysis of the experimental results provides a detailed description of the competing mechanisms leading to an ignition or a lack of ignition of the target tree.

1. Introduction

Even as detailed physical models of wildland fire spread have been constantly developed and improved in the last 25 years [1], there is still a significant barrier to the use of physical models as tools supporting the needs of fire managers, urban planners and firefighters. The main tools used by end users are based on empirical models [2]. Several factors can be identified that make up the barrier for physical models, such as the computational cost of running complex models, the high level of technical skills necessary to use them, and the multitude of parameters that are needed to implement them. However, the main reason resides in the gap in knowledge that still exists in our understanding of the basic mechanisms that drive wildfire spread and how these mechanisms interact together [3]. In the recent past, several studies have focused on the mechanisms of fire spread [4], including the processes leading to particle heating [5,6] and the role of buoyant flames [7]. The studies have focused on fire spread through litter [8] or deep fuel beds [9]. Many times, the studies have highlighted the role of convection, either to cool [5] or heat up [5–9] the flames.

While in the past, a strong focus has been on radiation in order to develop simplified fire spread models [10,11], the recent attention on convective transfer has inversed this trend. Recognizing that heat transfer can happen through convection and radiation during fire spread [4,8], this work aims at contributing to a better understanding of the role of radiative heat transfer. When a fuel element is heated, several parameters contribute to the heating. Some are linked to the fire (flame geometry, fire front width, residence time, etc.) and some are linked to the fuel element (fuel moisture content, bulk density, particle shape, absorptivity, etc.).

Several studies used idealized fuels that are made of industrially-processed fuels extracted from vegetation, such as excelsior or cardboard [5,7–9]. In our study, trees in their natural state were used to obtain fuel and fire conditions as close to reality as possible. Indeed, vegetative fuels have complex geometries and their foliage is made of complex compounds that are not all present in industrially-processed fuels, while they can have a strong influence on flammability [12]. A convenient way to isolate the role of radiative transfer is by creating discontinuous fuels [9]. Such fuels are present in the natural environment, leading to threshold behavior in fire spread [13,14].

Our study aimed to observe the physical phenomena and decompose the mechanisms of fire spread through a gap in fuels, without flame contact. We used a group of three trees that were simultaneously ignited and a target tree located at a small distance from the grouped trees. The target tree was instrumented to capture heat transfer and temperature. The gap between the grouped trees and the target tree was designed to ensure that no flame contact or significant hot gas contact occurred. The

* Corresponding author.
E-mail address: asimeoni@wpi.edu (A. Simeoni).

https://doi.org/10.1016/j.firesaf.2020.103066
Received 10 January 2020; Accepted 28 April 2020
Available online 3 May 2020

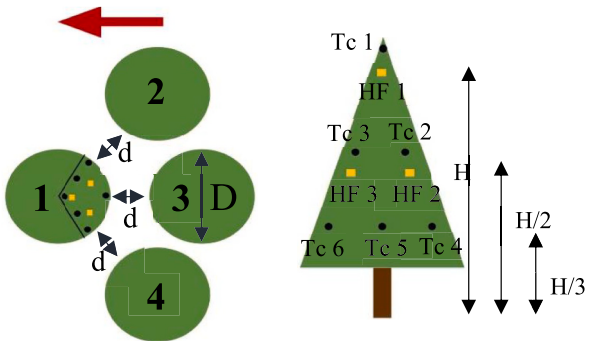

Fig. 1. a). Top view of the experimental layout, b) Side view of the target tree.

ignition conditions of the target tree were recorded and some of the mechanisms leading to ignition or no ignition were described, highlighting when radiant transfer can lead to the ignition of discontinuous fuels for no-slope and no-wind conditions.

2. Materials and Methods

The experiments were designed to examine if, and under what conditions, radiation could be responsible for fire spread through a gap between fuels. The experiments consisted of four Douglas fir trees, three of them being ignited with three gas burners, and a target tree a prescribed distance from the others (Fig. 1). The size of the gap, either 25 or 30 cm from the widest point of the trees, was set to ensure that there would not be any contact between the flames and the tree, to favor radiative transfer and to limit the influence of convective transfer on the fire spread. The set of experiments consisted of nine tests. Specific conditions favorable to fire spread were chosen: no slope, no wind, a moisture content below 30%, and small gaps. The trees were grouped by size: smaller trees were first used, followed by bigger ones. The main variations between trees were about size and bulk density. Incident heat fluxes, and temperatures were measured to estimate the thermal conditions for successful and unsuccessful ignition of the target tree, with sensor locations shown in Fig. 1.

One of the long-term goals of this study is to provide data useful for CFD models of fire spread. Hence, Douglas fir has been selected for the sake of consistency with a previous CFD study on burning single trees and the fact that most of the fuel properties have been measured [15].

The trees were freshly cut at a nearby Christmas tree farm. To reach conditions favorable for fire spread and for ignition of the target tree [16–18], the trees were dried in a custom-built oven for 12 h at 50 °C. This resulted in needle moisture contents below 30%.

Because of laboratory conditions, we were limited to trees with a maximum height of 2.3 m. We compensated for the smaller radiative impact compared to the one expected for fire in fully-grown trees in the field with the low fuel moisture content described above. Indeed, the non-linear properties of radiative transfer make scaling down large wildland fire front particularly challenging [19]. Another way to

Table 1
Summary of the experiments.

		Experiment Number	Tree Number	Δm (kg)	Mass Loss Rate (kg/s)	Moisture content (%)	Distance between source and target trees (cm)	Tree alignment	Target tree ignition
Small trees	Low density	1	1	x	x	14	30	Line	No
			2	1.14	0.05	10			
			3	x	x	13			
			4	1.4	0.07	8			
		2	1	x	x	7	30	Line	No
			2	2.97	0.095	11			
			3	x	x	9			
			4	x	x	13			
		3	1	x	x	17	25	Curved	**Yes**
			2	1.59	0.07	14			
			3	x	x	15			
			4	x	x	8			
		4	1	x	x	19	25	Curved	No
			2	2.21	0.098	18			
			3	x	x	14			
			4	x	x	17			
	High density	5	1	x	x	34	25	Curved	No
			2	3.94	0.17	31			
			3	x	x	38			
			4	2.03	0.15	20			
Large trees		6	1	x	x	11	25	Curved	**Yes**
			2	3.63	0.146	11			
			3	x	x	11			
			4	x	x	12			
		7	1	x	x	10	25	Curved	No
			2	x	x	8			
			3	2.26	0.125	10			
			4	x	x	10			
		8	1	x	x	10	25	Curved	**Yes**
			2	3.86	0.16	11			
			3	3.21	0.17	12			
			4	x	x	10			
		9	1	x	x	14	25	Curved	**Yes**
			2	x	x	13			
			3	3.29	0.16	10			
			4	x	x	11			

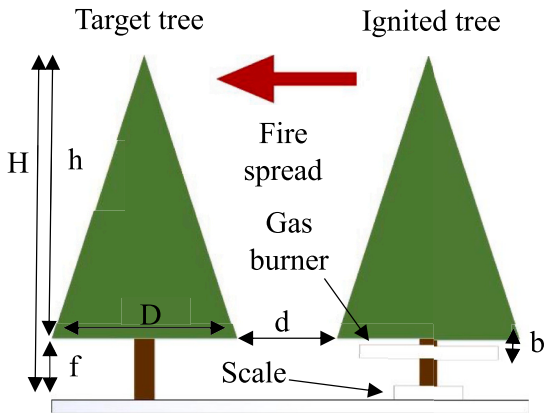

Fig. 2. Side view of the experiment.

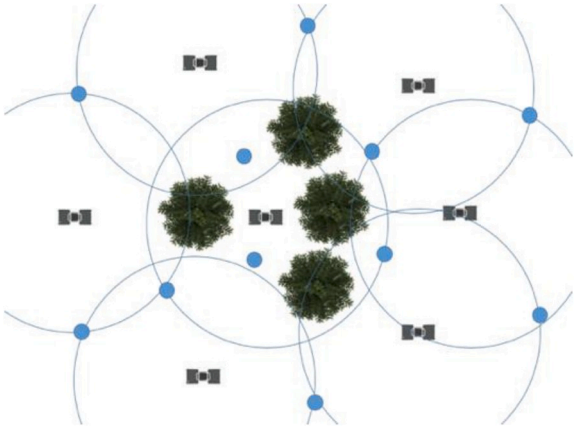

Fig. 3. Position of the TLS system and reference targets.

compensate is by having relatively small gaps while still ensuring no flame contact. A rough estimation of the peak heat release rate is between 3 and 9 MW for the 3 grouped trees. This estimation is based on the peak mass loss rate for the burning trees measured in this work and the contribution to the heat released by the flames only (and not by the char oxidation) using the method developed in Ref. [15], which also tested Douglas firs.

Tree 1 in Fig. 1a is the target tree. It was placed at a distance d, representing the gap with trees 2, 3 and 4. Trees 2, 3 and 4 were placed first in a line and then in a curve to increase the view factor and maximize the fire spread potential due to radiation (see Table 1).

The target tree was equipped with tree pairs of one total (water-cooled Schmidt-Boelter gauge, 0.94 absorbance, 3% uncertainty) and one radiative (water-cooled Gardon gauges with a sapphire window, 0.92 absorbance, 3% uncertainty) heat flux meters. Pair 1 was placed at the top of the target tree while pairs 2 and 3 were placed side-to-side, at the mid-height of the tree (see Fig. 1b). The heat flux meters were oriented to match the inclination of the outer shape of the foliage. The target tree was equipped with six thermocouples (type K exposed junction, 24-gauge wire, diameter 0.51 mm, bead diameter 0.71 mm), set to cover most of the tree side facing the fire (see Fig. 1). The thermocouples were mounted to be hidden by the needles and great care was taken to avoid direct exposure to the flames from the other trees, to best represent the conditions inside a bunch of needles. All data was acquired at a frequency of 1Hz.

The grouped trees (trees 2, 3 and 4) were set on fire with three ring-shaped gas burners positioned under their crown as shown on the bottom right of Fig. 2 [15]. Each gas burner released approximately 30 kW. For each experiment, two scales were positioned under trees 2 and 4 to

Table 2
Tree geometry for successful ignitions.

Experiment Number	Tree	Tree Height (m)	Crown Base Height (m)	Crown Width (m)	Tree Volume (m^3) – Voxel Size 0.1 cm^3
3	1	1.772	0.107	0.974	0.805
	2	1.295	0.141	0.993	0.791
	3	1.759	0.053	0.939	0.741
	4	1.401	0.183	1.025	0.673
6	1	1.984	0.083	1.281	1.347
	2	1.797	0.221	1.175	1.156
	3	2.003	0.224	0.776	1.248
	4	1.773	0.11	1.103	1.271
8	1	1.806	0.197	1.121	1.474
	2	1.776	0.141	1.102	1.264
	3	2.343	0.088	1.229	1.376
	4	2.057	0.08	1.302	1.912
9	1	1.909	0.078	1.008	1.538
	2	1.869	0.038	1.248	1.748
	3	2.15	0.1	1.288	1.938
	4	1.821	0.107	1.554	2.306

record the mass loss rates. The trees were ignited in succession, starting by tree no. 4. All were ignited in a 2 s interval. All the instruments were synchronized before the start of each experiment.

A set of three-dimensional scans were collected using a Terrestrial Laser Scanner (TLS; FARO® Focus^S LIDAR) in order to characterize the structure of the trees and to archive instrument locations. Each experimental setup was scanned from seven positions before and after each burn. For spatial referencing, needed to mosaicking of the individual scans into a single scene, reference targets, were placed in positions around the trees where they would be recorded in multiple scans. Fig. 3 shows the position of the scanner and reference targets, that allowed the tree dimensional reconstruction of the experimental layout. The scans were later compiled in one 3D point cloud using the FARO Scene software. The TLS data was used to provide the geometry of the trees for successful ignitions. The volume was estimated through a 3-D voxel-based approach [20].

The experiments were recorded with six GoPro cameras. Two cameras were positioned on each side of the gap between trees, three cameras were located under the target tree, and another camera was positioned right above the target tree (as can be seen in Fig. 5). This last camera was encased in a box to be protected from the heat generated by the flames. This setup offered many view angles and ensured that we could verify that there was no flame contact in case of fire spread to the target tree.

The moisture content was measured for each tree. Five minutes before each burn, samples of needles and small branches ($\varnothing < 5\,mm$) were collected at various positions in each tree. Then, they were weighted, left in an oven for 24 h at 60 °C and weighed again. The following formula (1) was used, which corresponds to the fuel moisture content on a dry basis:

$$M = \frac{m_{e,wet} - m_{e,v}}{m_{e,v}} * 100 \quad (1)$$

With: $m_{e,wet}$ = Mass before drying.

$m_{e,v}$ = Mass after drying.

Table 1 shows all the experiments carried out, the type of tree alignment, the spacing between trees, the moisture content, as well as the ignition conditions. For the first two experiments, the trees were positioned in a single line with a spacing of 30 cm between the line and the target tree. For all the other experiments, the trees were positioned in a curve with a spacing of 25 cm. For each experiment, the trees were selected to have close geometrical features. For experiments 3 and 4, the trees were small (around 1.20 m) with a low density. For experiment 5,

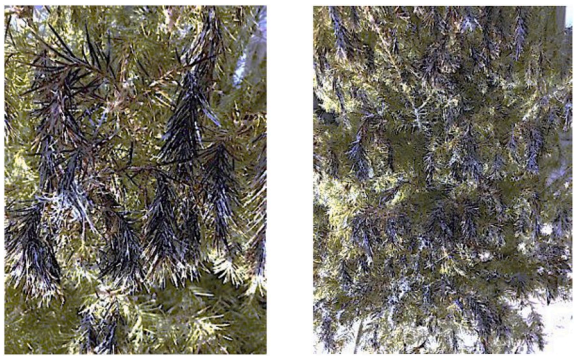

Fig. 4. Views of experiment 5 after the smoldering phenomenon.

Fig. 5. Pyrolysis gases, experiment 8 (target tree is 1.8 m high, see Table 2).

the trees were small (around 1.20 m) with a high density. And for experiments 6 to 9, the trees were big (around 2 m) with a high density, see Table 2.

Table 2 provides the geometry of the trees for the experiments with successful ignition of the target tree. At this stage, the local bulk density has not been measured but an estimation of the volume of the trees has been provided from the LIDAR data by using the voxel-based approach [20]. The average bulk density of the burned (and thinnest) particles can be inferred from the mass lost and the volume of the tree [15].

3. Results

The experiments can be split into two categories: fire spread to the target tree or no fire spread. No flame contact was observed in any of the experiments, based on the videos recorded by the 6 video cameras located around the target tree. Without flame contact, the strong buoyancy created by the three burning trees prevented hot gases to cross the space between the flames and the target tree. Hence, it is assumed that fire spread overall, could only happen because of radiative transfer. The fire was able to spread four times (44% of the time). For the remaining five tests, or 56% of the cases, the target tree did not ignite. However, a quite significant smoldering phenomenon was observed on the outer shape of the target tree as demonstrated by the remaining ash and char seen in Fig. 4 that shows two different views of the smoldering phenomenon on the target tree after completion of experiment 5.

As shown in Table 1, no target tree was ignited for the linear alignments and the 30 cm separation distance. For the smaller trees (experiments 3 to 5), one in three cases, or 33%, caught fire. It corresponded to the drier trees in the curved alignment (experiment 3). Experiment 5, while having denser trees, did not ignite, likely because the trees had the higher moisture content. For the largest trees (experiments 6 to 9) three in four cases, or 75%, ignited.

The large flames and the high radiation led to the production of pyrolysis gases at the exposed edge of the target tree, as seen in Fig. 5. It should be noted that the pyrolysis gases of the target tree expand towards the burning trees, showing the absence of flame contact. The gas production directly relates to radiation but also depends on the density of the trees as well as the composition of the gas. Finally, the moisture content also plays a role in the production of pyrolysis gases by delaying their release and diluting them. A fuel moisture below 30% in conifers generally leads to short ignition times in the range of heat fluxes measured here (around 50 kW/m^2) [15–17].

In another study [21] smoldering happened before flaming ignition for solid wood elements. It also mentioned the effects of cooling and diluting the pyrolysis gases to explain the delay between smoldering and flaming ignition. In the case of vegetation, an additional effect of cooling of the thinnest particles by the flow may also be contributing to the lack of transition from smoldering to flaming [18].

In the current setup, we were not able to fully capture the ignition process. The video cameras showed that ignition happened at the tip of branches but it is unclear if those tips were smoldering or not beforehand. At this stage, it is impossible to say with certainty if the ignition was due to a transition from smoldering to flaming or if it was through auto-ignition in the gas phase. This aspect deserves further investigation in the future.

Figs. 6–10 present the values of the temperatures and heat fluxes for

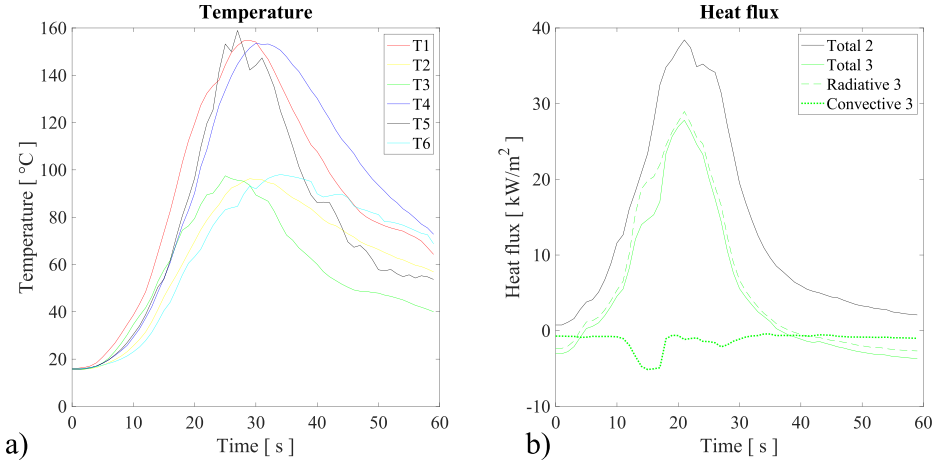

Fig. 6. Experiment 1 – a) Temperature, b) heat flux distributions.

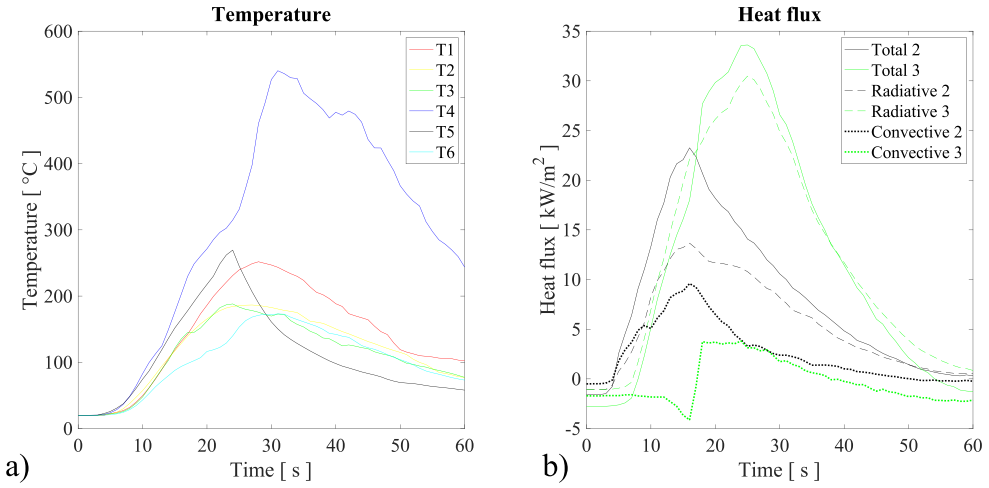

Fig. 7. Experiment 5 – a) Temperature, b) heat flux distributions.

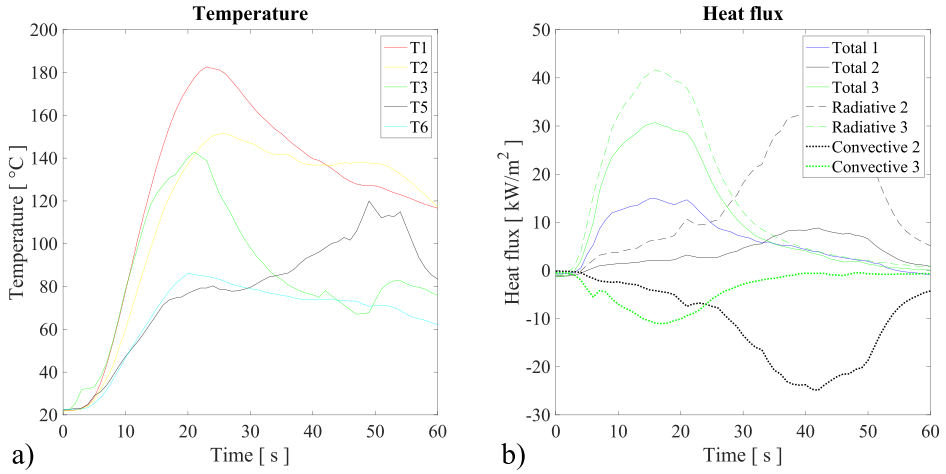

Fig. 8. Experiment 7 – a) Temperature, b) heat flux distributions.

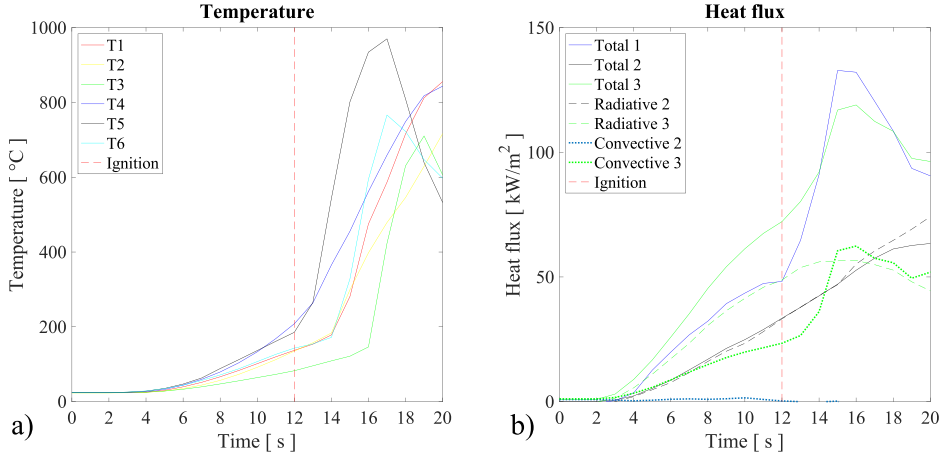

Fig. 9. Experiment 8 – a) Temperature, b) heat flux distributions.

experiments 1, 5, 7, 8 and 9. These experiments were chosen to present all the types of observed behavior. Fig. 6 shows no ignition for the line alignment and the 30 cm separation distance during experiment 1. For the curved alignment and the 25 cm separation distance, Figs. 7 and 8 present no ignition with smoldering and Figs. 9 and 10 present flaming ignitions (see Table 1).

These figures highlight different mechanisms. First, Figs. 6b to 10b show that flaming ignition of the target tree only happened if one of the heat flux sensors recorded radiative heat fluxes above 50 kW/m^2 (below this value for Figs. 6b-8b and above this value for Figs. 9b and 10b). This

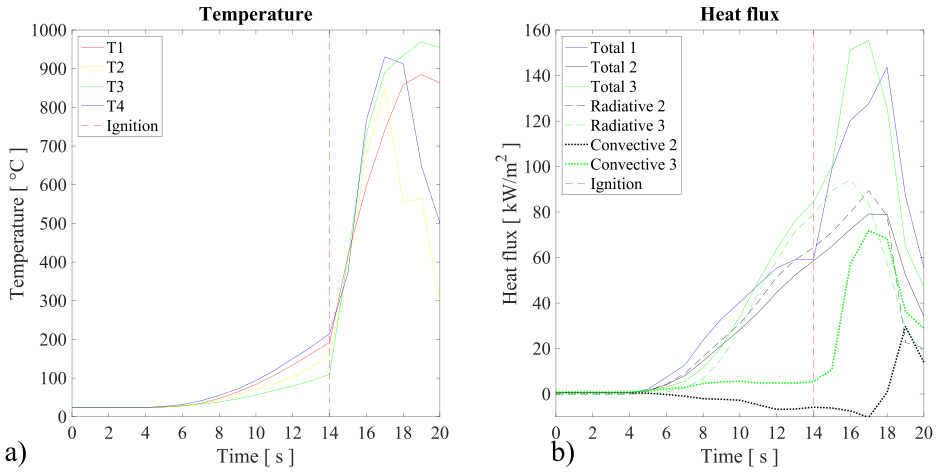

Fig. 10. Experiment 9 – a) Temperature, b) heat flux distributions.

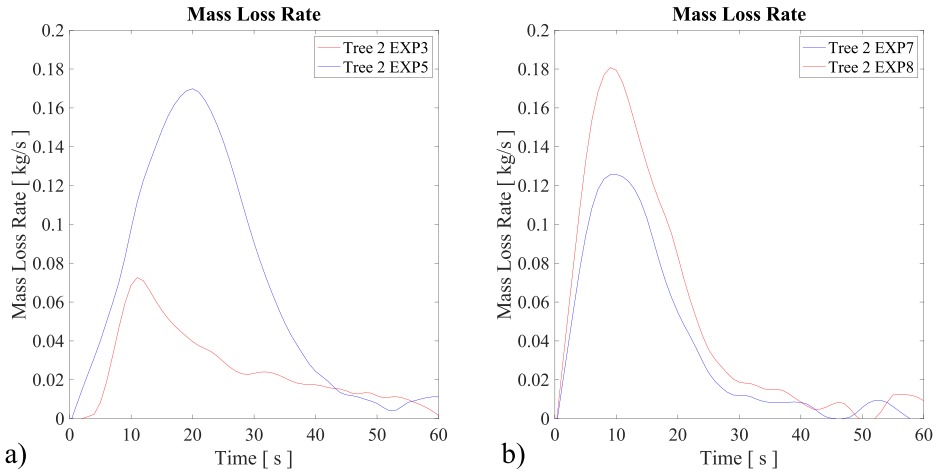

Fig. 11. Mass loss rate of the ignited trees for ignition (red) and no ignition (blue) experiments. (For interpretation of the references to colour in this figure legend, the reader is referred to the Web version of this article.)

value corresponds to the incident flux on the needles located on the outer shape of the exposed side of the trees measured at the location of the heat flux meters (see Fig. 1b). It should be noted that this value has been found to be the value reached by the fuel before ignition during fire spread in the field [4]. For all the experiments undergoing ignition, the ignition times were between 10 s and 20 s. The heat flux values correlate well with the temperature values. Indeed, Figs. 9a and 10a show the ignition at a sharp transition on a few seconds, from 200 °C to 1000 °C. The peak temperature is consistent with the literature for field experiments of fires spreading in forest stands [22]. However, the temperature of 200 °C at ignition is lower than the typical ignition of solid fuels [16]. This is due to the fact that the recorded temperatures at ignition are not at the exact ignition location (see Fig. 14). This comment also applies to the measured heat fluxes, making the heat flux and temperature values only indicative of a minimum exposure but not representative of the local ignition conditions.

Fig. 8 show a late peak for the temperature and the heat flux. This is due to the fact that this particular experiment had an issue with its ignition process and the tree facing HF2 (see Fig. 1b) had a delayed ignition.

In addition, none of the 6 video cameras showed any flame contact but Figs. 7 and 9 show a substantial convective heating at one of their location and Fig. 10 shows a low convective heating at one of its locations. This can be understood by describing the dynamics of the experiments: when the 3 trees are ignited, a very strong draft is created by buoyancy that sucks the air all around those trees, mainly leading to convective cooling (all the other locations and all the other figures display convective cooling). However, as the heat flux sensors were positioned on the higher half of the tree (see Fig. 1b), it is possible and even likely that some of them were in contact with the degradation gases (water vapor and pyrolysis gases) before ignition and then experienced convective heating. It is also possible that smoldering happening below the heat flux sensors heated the air sufficiently to induce additional convective heating. Among the experiments with no ignition, experiment 5 (Fig. 7) is the one that saw the most smoldering. It is also the experiment where the target tree had a higher moisture content (20%, see Table 1). We have no direct explanation for the strong convective heating in experiment 8 (Fig. 9), which is an outlier for the experiments with ignition and this effect will have to be studied further in the future. However, we propose that the convective heating is a secondary phenomenon that is a consequence of the radiative heating of the tree and it is not driving ignition.

Fig. 11a shows a comparison of the mass loss rates of one the ignited trees between experiments 3 and 5. As a reminder, experiment 3 ignited but experiment 5 did not. However, the mass loss rate is significantly higher for experiment 5 and, the exposition is much longer. This is due to the fuel moisture content. Indeed, in experiment 3, the fuel moisture content is 14% against 31% in experiment 5 (Table 1), so experiment 5 has a larger mass loss but it is mainly made of water.

Fig. 11b shows a comparison between the mass loss rates of

Fig. 12. Embers and pyrolysis gases during experiment 5 (no spread).

Fig. 13. Position of TC 4 for experiment 5.

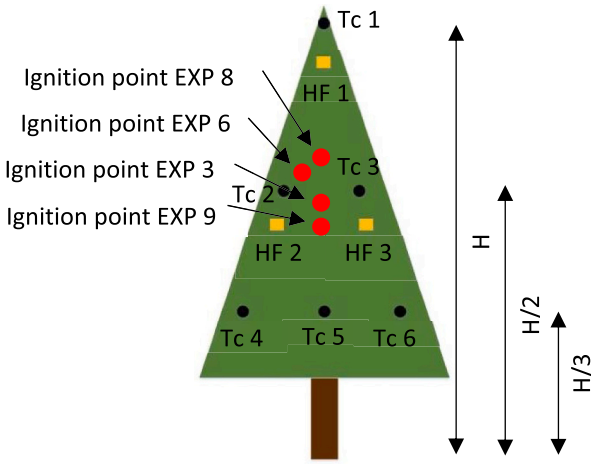

Fig. 14. Position of ignitions.

experiments 7 and 8 for the ignited trees. For the two experiments, the fuel moisture content is quite similar (see Table 1) but experiment 8 ignited and experiment 7 did not. The mass loss rate for experiment 8 is higher, which is consistent with a larger radiative impact from the burning trees, given the fact that the fire has spread. Concerning experiment 7, the delayed ignition of one tree is certainly responsible of a lower radiative impact on the target tree but a strong cooling is measured in two locations (see Fig. 8), and it certainly contributed to prevent the fuel vapor released by the target tree to ignite (see also later discussion and Fig. 15).

It has already been highlighted that convective heating plays an important role in fire spread [7]. In these experiments, convective cooling coming from the lower part of the tree played an opposite role by cooling the pyrolysis gases and the tree itself, and delaying the ignition phenomenon. A strong draft created by buoyancy has been observed visually and at many angles with the cameras. In addition, the supply of fresh air also diluted the gases, lowering their concentration and decreasing the possibility of auto-ignition in the gas phase, and even of piloted ignition in the presence of smoldering [23]. In Fig. 8 (experiment 7 which did not ignite), the convective cooling is much larger than in Fig. 9 (experiment 8 which ignited). This effect is directly related to the bulk density of the tree. Indeed, the denser the tree, the harder for the fresh air to pass through and therefore cool the needles and to cool and dilute the gases. This can even reverse the trend by allowing the degradation gases and the smoldering products to heat other parts of the tree as they will experience less dilution (see previous discussion of convective heating in Fig. 9). Hence, the ignition of the tree and therefore the fire spread will be easier for experiment 8.

For the smoldering experiments, despite the appearance of embers (see Fig. 12) and a substantial presence of pyrolysis gas, the target tree did not ignite. This phenomenon is directly related to the buoyant flow, which will dilute and cool the gases, cool the needles, and activate glowing combustion. The density of the tree will influence this phenomenon by allowing fresh gases to penetrate or not into the tree.

In experiment 5, thermocouple 4 captured the smoldering as its peak temperature exceeded 500 °C (see Fig. 7a) while the others remain around 200 °C. Fig. 13 shows the location of this thermocouple in an area of the tree affected by smoldering (presence of ash).

Fig. 14 shows the position of the different ignitions. Despite the same experimental layout, the ignition happened at different locations and we visually confirmed that those locations were denser parts of the trees, where branches were close to each other. This observation supports the assumption on the role of density in the ignition process but direct measurements of the local bulk density will be necessary to confirm them.

From all these observations, several explanations emerge that highlight the three main factors influencing the ignition conditions:

- The gap: radiative transfer depends greatly on distance, here corresponding to the gap. None of the configurations with line alignment and the larger gap ignited (see Table 1).
- The local and mean bulk densities of the target tree: the density of the target tree will directly influence the ability of the convective flow to penetrate the tree and cool and dilute the pyrolysis gases. In addition, the density of the tree foliage will influence how much radiation is absorbed on the exposed side of the tree.
- Fuel moisture content: This parameter has a direct influence on the ignition of the tree. Flaming ignition is strongly dependent on fuel moisture content. For instance, a small sample of live needles with a fuel moisture content around 50% have displayed a time to ignition of 59 s when submitted to a 50kW/m2 radiative heat flux [17]. This time is significantly higher than the burning time of the grouped trees measured in this work (30 s in average). This effect was confirmed during the smaller tree experiments for the curved alignments. For the three tests with very similar types of trees, the one with a value of 17% ignited, experiment 3, while the one with a

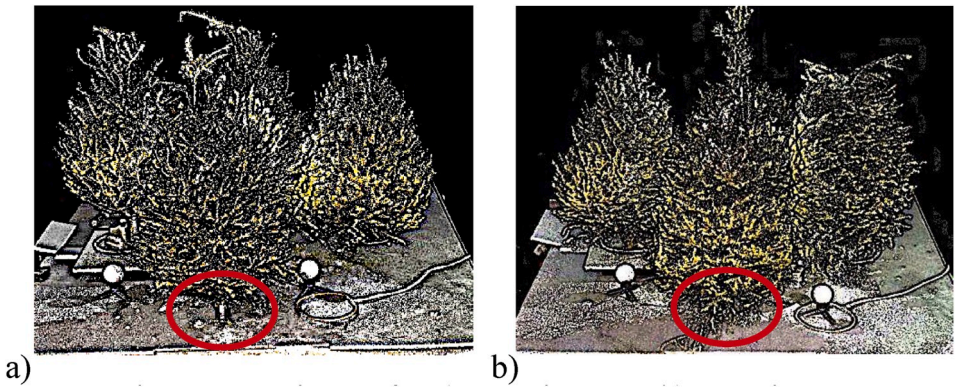

Fig. 15. TLS image for a) experiment 7, b) experiment 8.

value of 34% did not ignite, experiment 5, and instead produced a strong smoldering.

All the parameters presented above allow us to propose explanations on why some trees caught fire while others did not:

- In the case of the 30 cm and line alignment, maybe the view factor was too small because the flames generated by tree 2 and 4 were further away from the target tree.
- In the case of the 25 cm and curved alignment with the small trees (experiments 2 to 5), the target tree used for experiment 4 was probably not dense enough. The one from experiment 5 may have been too wet.
- In the case of the 25 cm and curved alignment with the big trees, the target trees were rather dense but one was strongly pruned at its lower part. This facilitated the arrival of fresh air and thus, the cooling and dilution of gases by the convective flow. This can be seen in Fig. 15. Fig. 15a shows experiment 7 (also shown in Fig. 8), where the naked trunk of the target tree can be seen, while the one in experiment 8 (also shown on Fig. 9) remains hidden as seen in Fig. 15b. Experiment 7 did not ignite, while experiment 8 did ignite.

4. Conclusions

In this work, the fire spread through a gap by radiation and without flame contact, was studied. Nine experiments with a total of 36 trees were carried out. Out of the nine experiments, four propagated to the target tree. This research constitutes a preliminary step in a program dedicated to the study of fire spread through discontinuous fuels. However, a few important points were highlighted and will be the subject of further studies:

- Convection can play the role of diluting and cooling the pyrolysis gases, as well as cooling the unburned fuel.
- The local and average densities of the tree have a direct impact on the production of pyrolysis gases and the penetration of the convective flow into the tree itself.
- Fuel moisture content has a major damping effect for the burning rate, consecutively limiting the fire spread through the gap.
- The gap between trees leads to a threshold behavior that can be explained by a combination of factors.

As for all preliminary studies, some improvements are needed to better quantify the effects that were observed. Techniques for characterizing fuels at fine scale must be resolved in order to further understand the effects of drag on convective processes. For instance, we were only able to use the TLS to confirm the 3D layout but it has the potential to bring more quantification of the tree bulk density [24]. In addition, it is important to remember the complexity of developing a large-scale testing program, as well as the stress the instrumentation undergoes during massive heat exposure. Conducting a full experimental program by burning several trees at once is very time and energy consuming. However, these experiments lay the ground for complementary smaller scale studies and CFD simulations in order to better isolate and represent the observed phenomena.

Declaration of competing interest

The authors declare that they have no known competing financial interests or personal relationships that could have appeared to influence the work reported in this paper.

References

[1] D. Morvan, Physical phenomena and length scales governing the behaviour of wildfires: a case for physical modelling, Fire Technol. 47 (2011) 437–460.
[2] A.L. Sullivan, Wildland surface fire spread modelling, 1990–2007. 2: empirical and quasi-empirical models, Int. J. Wildland Fire 18 (2009) 369–386.
[3] M.A. Finney, J.D. Cohen, S.S. McAllister, W.M. Jolly, On the need for a theory of wildland fire spread, Int. J. Wildland Fire 22 (2012) 25–36.
[4] F. Morandini, X. Silvani, Experimental investigation of the physical mechanisms governing the spread of wildfires, Int. J. Wildland Fire 19 (2010) 570–582.
[5] J.D. Cohen, M.A. Finney, An examination of fuel particle heating during fire spread, in: 6th International Conference on Forest Fire Research, 15-18 November, Coimbra, Portugal, 2010.
[6] S. McAllister, M. Finney, Autoignition of wood under combined convective and radiative heating, Proc. Combust. Inst. 36 (2) (2017) 3073–3080.
[7] M.A. Finney, D. Cohen Jack, M. Forthofer Jason, S. McAllister Sara, J. Gollner Michael, J. Gorham Daniel, Kozo Saito, K. Akafuah Nelson, A. Adam Brittany, D. English Justin, Role of buoyant flame dynamics in wildfire spread, Proc. Natl. Acad. Sci. Unit. States Am. 112 (32) (2015) 9833–9838.
[8] X. Sánchez-Monroy, W. Mell, J. Torres-Arenas, B.W. Butler, Fire spread upslope: numerical simulation of laboratory experiments, Fire Saf. J. 108 (2019) 102844.
[9] M.A. Finney, J.D. Cohen, I.C. Grenfell, K.M. Yedinak, An examination of fire spread thresholds in discontinuous fuel beds, Int. J. Wildland Fire 19 (2010) 163–170.
[10] H.M. Cekirge, Propagation of fire fronts in forests, Comput. Math. Appl. 4 (4) (1978) 325–332.
[11] F.A. Albini, Wildland fire spread by radiation-a model including fuel cooling by natural convection, Combust. Sci. Technol. 45 (1–2) (1986) 101–113.
[12] W.M. Jolly, D.M. Johnson, Pyro-ecophysiology: shifting the paradigm of live wildland fuel research, Fire 1 (2018) 8.
[13] J. Nahmias, H. Téphany, J. Duarte, S. Letaconnoux, Fire spreading experiments on heterogeneous fuel beds. Applications of percolation theory, Can. J. For. Res. 30 (2000) 1318–1328.
[14] A. Simeoni, P. Salinesi, F. Morandini, Physical modelling of forest fire spreading through heterogeneous fuel beds, Int. J. Wildland Fire 20 (5) (2011) 625–632.
[15] W. Mell, A. Maranghides, R. McDermott, S.L. Manzello, Numerical simulation and experiments of burning Douglas fir trees, Combust. Flame 156 (10) (2009) 2023–2041.
[16] V. Babrauskas, Ignition of wood: a review of the state of the art, J. Fire Protect. Eng. 12 (3) (2002) 163–189.
[17] F.X. Jervis, G. Rein, Experimental study on the burning behaviour of *Pinus halepensis* needles using small-scale fire calorimetry of live, aged and dead samples, Fire Mater. 40 (2016) 385–395.
[18] J.C. Thomas, Improving the Understanding of Fundamental Mechanisms that Influence Ignition and Burning Behavior of Porous Wildland Fuel Beds, PhD Thesis, University of Edinburgh, UK, 2017.
[19] J.G. Quintiere, Scaling applications in fire research, Fire Saf. J. 15 (1) (1989) 3–29.

[20] Rowell E., Loudermilk E.L., Hawley C., Pokswinski S., Seielstad C., Queen L., O'Brien J.J., Hudak A.T., Goodrick S., Hiers J.K. Coupling Terrestrial Laser Scanning with 3D Fuel Biomass Sampling for Advancing Wildland Fuels Characterization. bioRxiv 71469; doi: https://doi.org/10.1101/771469.
[21] R. Bilbao, J.F. Mastral, M.E. Aldea, J. Ceamanos, M. Betrán, J.A. Lana, Experimental and theoretical study of the ignition and smoldering of wood including convective effects, Combust. Flame 126 (1–2) (2001) 1363–1372.
[22] E.V. Mueller, N. Skowronski, J.C. Thomas, R.M. Hadden, W. Mell, A. Simeoni, Local measurements of wildland fire dynamics in a field-scale experiment, Combust. Flame 194 (2018) 452–463.
[23] A.B. Dodd, C. Lautenberger, C. Fernandez-Pello, Computational modeling of smolder combustion and spontaneous transition to flaming, Combust. Flame 159 (1) (2012) 448–461.
[24] N.S. Skowronski, S. Haag, J. Trimble, K.L. Clark, M.R. Gallagher, R.G. Lathrop, Structure-level fuel load assessment in the wildland–urban interface: a fusion of airborne laser scanning and spectral remote-sensing methodologies, Int. J. Wildland Fire 25 (2015) 547–557.